Analysis of Synthetic Cylindrical Array Beam-Forming in Presence of the Elements Position-Error for Semi-Anechoic Chamber Evaluation

Karlisa Priandana #1, Mir Ghorashi #2, Jun-Ichi Takada #3,
Michitaka Ameya *4, Satoru Kurokawa *5, Masanobu Hirose *6

#International Development Engineering, Tokyo Institute of Technology
S6-4, 2-12-1, O-okayama, Meguro-ku, Tokyo 152-8552, Japan
{1lisa, 2mir, 3takada}@ap.ide.titech.ac.jp
*National Institute of Advanced Industrial Science and Technology
1-1-1, Umezono, Tsukuba, Ibaraki 305-8563, Japan
{4m.ameya, 5satoru-kurokawa, 6masa-hirose}@aist.go.jp

***Abstract*—This paper describes the study of synthetic cylindrical array beam-forming for narrowband signals, under the influence of antenna elements position-error. The required side-lobe level and the physical dimensions of the array are presumed based on the requirements and limitations to evaluate a RF semi-anechoic chamber. Dolph-Chebyshev algorithm is used for beam-forming because of its optimal beam-width for a predefined uniform side-lobe level. Monte-Carlo simulations reveal the sensitivity of the beam-pattern side-lobe level to the elements position-error.**

***Index Terms*—Beam-forming, beam-width, synthetic cylindrical array, Davies transformation, Dolph-Chebyshev, Monte-Carlo, semi-anechoic chamber, side-lobe, super-directivity**

I. Introduction

The rapid emergence of electromagnetic (EM) equipments has forced us to carefully conduct the electromagnetic compatibility (EMC) testing, to avoid the possibility of interference. Ideally, EMC testing is conducted in an open-area test site (OATS), an obstacle-free environment. However, it is inconvenient due to the high dependency on the changing factors of the environment. As a result, EMC test is conducted inside a semi-anechoic chamber (SAC): a room having walls and a ceiling equipped with EM absorbers, and a metallic ground. To simulate an OATS, SAC should be free from scattering waves other than the ground-reflected wave. However, in reality, the imperfect absorbers, corners, junctions, etc., may cause the SAC discrepancy from an ideal OATS. Therefore, evaluation of SAC is required.

Standardized validation methods to evaluate the SAC have been developed by CISPR/A [1]. The validation is established by finding the Site VSWR (S_{VSWR}) of the SAC. Standing waves voltages are measured at discrete locations of receiving antenna, to vary the phase between the direct and scattering (unwanted) waves. S_{VSWR} is the ratio of the maximum voltage to the minimum voltage. For SAC of 1-18 GHz, the S_{VSWR} at each frequency of at least 50 MHz steps should be less than 2:1 (in linear scale) or 6 dB (in logarithmic scale). The disadvantage of this method is the inability to identify the reasons behind the SAC discrepancy from an ideal OATS. This is because the obtained output is only the S_{VSWR} with no other information about the source(s) of the scattering waves. Thus, the performance of SAC cannot be improved. Another limitation is that the frequency selective scattering may not be captured by this method due to the discretized sampling.

This paper proposes the utilization of beam-forming for SAC evaluation. This method require a similar measurement system with that of the standard Site VSWR method. However, different measurement positions will be used as a synthetic array antenna. This method offers an ability to identify the sources of SAC discrepancy by estimating the Angle-of-Arrival (AoA) of the detected signals. The frequency dependent scattering signals due to the frequency dependent reflections can also be detected. In this method, some assumptions are taken:

1) The chamber discrepancy occurs due to some scattering waves that are caused by discrete points inside the SAC. Each of these points is modeled as an independent signal source, to be identified by beam-forming.
2) The distance between receiving array antenna center and the scattering point(s) are far enough, so that the plane wave approximation can be applied. The near-field analysis will be incorporated by using the spherical-wave radiation in the future.
3) The estimated AoA information of each detected signal path will be enough to determine the origins of each scattering wave.

The final goal of this research is to design the applicable beam-forming methodology for SAC evaluation. In this study, a synthetic cylindrical array antenna will be used. The low side-lobe requirement for SAC evaluation is realized by using Dolph-Chebyshev algorithm. Monte-Carlo simulations were conducted to find the optimal array parameters that can produce minimum side-lobe level at reasonable beam-width, under the presumed antenna elements position-error.

II. Beamforming

The proposed SAC evaluation consists of a data measurement and a data analysis (beam-forming). The measurement apparatus is shown in Fig. 1. Only a single antenna element will be installed at each port of the vector network analyzer (VNA). A synthetic cylindrical aperture will be realized by moving the antenna at the receiver side, using a turn table and a step z-positioner. At each position, the transfer function within the frequency range of interest will be obtained from VNA. However, in the data analysis, each of the frequency transfer function will be separately analyzed. Note that the positioning error of the turn table and step z-positioner will cause some errors in the resultant synthetic cylindrical array due to the incorrect position of each antenna element.

Fig. 2 shows the geometry of a cylindrical array. In the figure, θ express the co-elevation angle, the angular deviation from

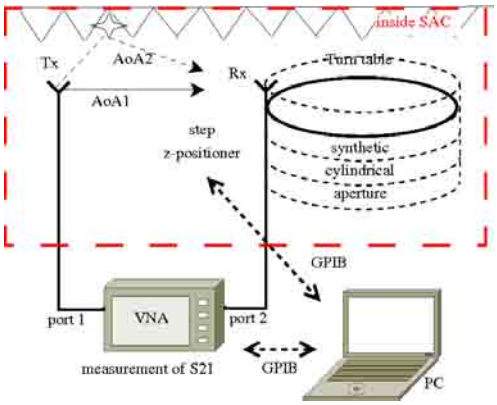

Fig. 1. Measurement Set-Up for SAC Evaluation

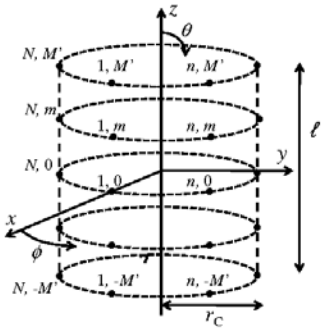

Fig. 2. Geometry of Cylindrical Array Antenna

the z-axis, whereas ϕ express the azimuth angle, the angular deviation from the x-axis at xy-plane. As can be seen from the figure, the array is composed of a uniform circular array (UCA) of N elements and uniform linear array (ULA) of M elements. Using the principle of pattern multiplication, the total pattern of the cylindrical array antenna is expressed as:

$$A(\theta,\phi) = A_{\mathrm{ULA}}(\theta)A_{\mathrm{UCA}}(\theta,\phi)F(\theta,\phi), \quad (1)$$

where:

$$A_{\mathrm{ULA}}(\theta) = \sum_{m=-M'}^{M'} w_m \exp(jkmd_{\mathrm{L}}\cos\theta), \quad (2)$$

$$A_{\mathrm{UCA}}(\theta,\phi) = \sum_{n=1}^{N} w_n \exp(-jkr_{\mathrm{C}}\sin\theta\cos(\phi-\phi_n)), \quad (3)$$

and $F(\theta,\phi)$ is the antenna element pattern, assuming that it is unchanged due to the rotation. In the equations, $k = 2\pi/\lambda$ is the wave-number of the incident wave, r_{C} is the UCA radius, N is the number of UCA elements, $M = 2M' + 1$ is the number of ULA elements, d_{C} is the circular interelement spacing, and d_{L} is the linear interelement spacing. The terms w_n and w_m express the weighting for the nth element of UCA and that for the mth element of ULA respectively.

Dolph-Chebyshev is a well known algorithm to design uniform side-lobe beam-patterns, with the narrowest beam-width for a predefined side-lobe level [3]. In its original format, it is only applicable to uniform linear array (ULA). To find the weighting for uniform circular array (UCA) of N elements, a preprocessing technique to transform its array manifold into a virtual ULA of size $N_{\mathrm{V}} = 2H + 1$ is required. The method is called *Davies Transformation*, which was first proposed by Davies in [4], and has been described briefly in [5]. A method to synthesize low side-lobe beam-patterns by adapting the Dolph-Chebyshev approach for a UCA is presented in [6] and [7]. The

TABLE I
SIMULATION VARIABLES

Variable		Value
signal frequency	f	$[1, 6]$ GHz
std of linear error	δd_{L}	1 mm
std of angular error	$\delta\phi$	0.1°
array height	l	$(M-1)d_{\mathrm{L}}$
array radius	r_{C}	$(Nd_{\mathrm{C}})/(2\pi)$
interelement spacing	d_{L}, d_{C}	$\leq 0.5\lambda$
defined side-lobe level	DSLL	-40 dB

transformation from UCA array manifold, $\mathbf{a}(\phi)$, to a virtual ULA array manifold, $\mathbf{a}_{\mathrm{V}}(\phi)$, can be expressed as:

$$\mathbf{a}_{\mathrm{V}}(\phi) = \mathbf{DTa}(\phi) = [\exp(-jH\phi), ..., 1, ..., \exp(jH\phi)]^T \quad (4)$$

where the elements of $\mathbf{T}$ are:

$$\mathbf{T}_{vn} = \exp(j2\pi nh/N), \quad (5)$$

n = 1, ..., N, v = 1, ... N_{V}, and h = -H, ..., 0, ..., H; and $\mathbf{D}$ is the normalizer diagonal matrix with elements:

$$\mathbf{D}_v = \left(Nj^h J_h(kr_{\mathrm{C}})\right)^{-1}, \quad (6)$$

where $J_h(\cdot)$ is the hth order Bessel function of the first kind.

The chosen of H has been described in [5] and [7] as:

$$H = \max_H \left\{ H \,\middle|\, H \leq \frac{N-1}{2},\ \frac{J_{H-N}(kr_{\mathrm{C}})}{J_H(kr_{\mathrm{C}})} < \epsilon \right\} \quad (7)$$

for some predetermined ϵ, which should be small enough (it was chosen as 0.05 in [7]) so that the obtained side-lobe level is equal to that determined in the Chebyshev polynomials).

III. SIMULATIONS AND DISCUSSION

Monte Carlo simulations, each of 10000 trials, were performed to find the mean MSLL under the influence of antenna elements position-error. The obtained mean MSLL at different array parameters (under the limitation of maximum array dimensions) were used to design the optimal parameters of synthetic cylindrical array with minimum MSLL at reasonable half-power beam-width (HPBW).

Table I shows the variables utilized in the simulation. The signal frequency ranges from 1 to 6 GHz. The antenna elements position-error were assumed as Gaussian-distributed random errors with standard deviation of 1 mm and 0.1° in linear and circular, respectively. To get the sufficient samplings of continuous antenna aperture, the maximum interelement spacings both in linear and circular, d_{L} and d_{C}, are limited to 0.5λ. Since the target specification of MSLL is -40 dB, the defined side-lobe level (DSLL) in Chebyshev polynomials was set to be -40 dB.

In the simulation, the investigation for elevation and azimuth beam patterns was separately conducted. The beam pattern in elevation mainly depends on the array factor of ULA (2) and antenna element pattern (assumed as ideal vertical dipole, $F(\theta) = \sin\theta$), whereas that in azimuth plane, i.e. $\sin\theta = 1$, merely depends on the array factor of UCA (3).

A. Uniform Linear Array

The first simulations were conducted to observe the elevation mean MSLL, μ_{MSLL}, in various linear interelement spacings, d_{L}, and number of elements, M, within the maximum physical array height of $l = 2$ m. The relation between elevation MSLL and d_{L} under the influence of antenna elements position error and their corresponding HPBW for f = 1 GHz and 6 GHz can be seen on Fig. 3 and Fig. 5. It is shown that the minimum achievable MSLL in $f = 1$ GHz is -36.8 dB (at $d_{\mathrm{L}} = 0.5\lambda = 15$ cm, $l = 1.8$ m,

and $M = 13$). In $f = 6$ GHz, -24.7 dB of minimum MSLL is obtained at $d_{\mathrm{L}} = 0.5\lambda = 2.5$ cm, $l = 0.3$ m, and $M = 13$. The different trends of MSLL with respect to d_{L} in Fig. 5 occur due to the different aperture size of the array.

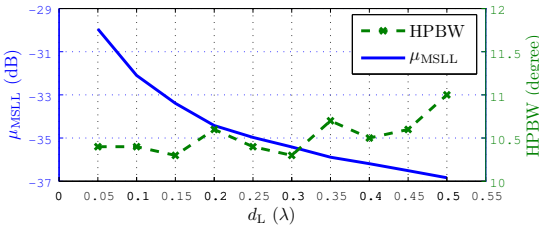

Fig. 3. Elevation Performance vs. d_{L} ($f = 1$ GHz, $l \simeq 2$ m)

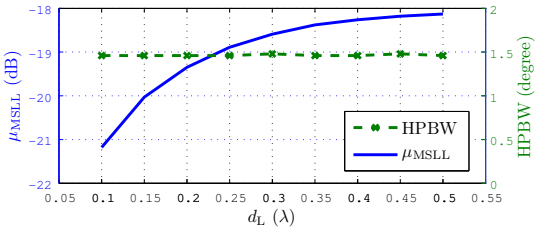

Fig. 4. Elevation MSLL and HPBW vs. d_{L} in $f = 6$ GHz at $l \simeq 2$ m

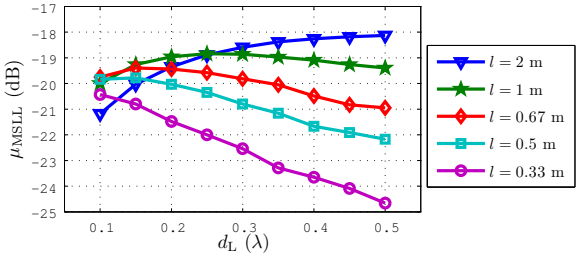

Fig. 5. Elevation MSLL vs. d_{L} ($f = 6$ GHz, Various l)

Based on these results, the optimal measurement sampling for the linear array at each frequency is: 13 points, with $d_{\mathrm{L}} = 0.5\lambda$. However, this scheme requires continuous measurement sampling as shown in blue dotted-line in Fig. 6. To save the calculation time, the measurement will be discretized. Sampling steps is determined by the highest frequency of 6 GHz, $d_{\mathrm{L}} = 2.5$ cm; whereas the total array height is determined by the lowest frequency of 1 GHz, $l = (M-1)d_{\mathrm{L}} = 1.8$ m. Thus, the linear aperture should be measured by 73 points, each 2.5 cm apart. At each point, all frequency transfer function of interest will be obtained.

In the data analysis, decimation technique will be applied. For each frequency of $f = [1, 6]$ GHz with 10 MHz steps, only 13 samples are taken with the corresponding linear spacings, d_{L}, shown in the green line in Fig. 6. Note that by implementing this scheme, the linear aperture l is electronically varied with respect to frequency. The expected performance in elevation for several frequencies of $f = [1, 6]$ GHz are shown in Fig. 7. It is shown that the range of elevation MSLL is $[-36.8, -24.7]$ dB, where higher MSLL is obtained at higher frequency, due to the linear error that are electronically larger. The elevation HPBW varied in the range of $11°, 20.4°]$ due to the different electronic aperture size, $l\,(\lambda)$. HPBW is inversely proportional to $l\,(\lambda)$ (as shown in Fig. 8), as expected.

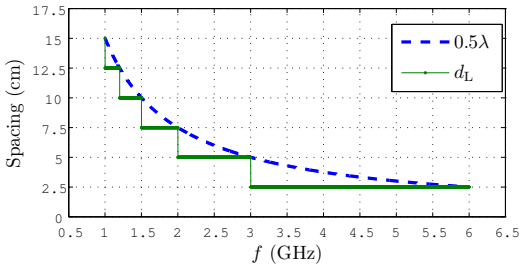

Fig. 6. Frequency vs. Linear Interelement Spacings

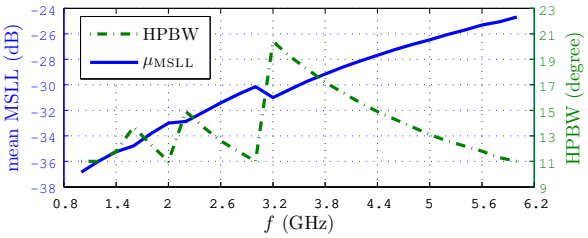

Fig. 7. Elevation MSLL and HPBW at $f = [1, 6]$ GHz

B. Uniform Circular Array

These simulations were conducted to observe the azimuth mean MSLL, μ_{MSLL}, in various circular interelement spacings, d_{C}, and number of elements, N, within the maximum physical array dimension of $r_{\mathrm{C}} = 0.5$ m. The relation between azimuth MSLL and d_{C} under the influence of antenna elements angular position-error for $f = 1$ GHz and 6 GHz can be seen on Table II and Table III. It was obtained that the minimum azimuth MSLL in $f = 1$ and 6 GHz are obtained by using a UCA of $r_{\mathrm{C}} = 0.5$ m with $N = 314$ and $N = 215$ respectively.

These two best measurement schemes are then compared in Fig. 9. The figure shows that the azimuth MSLL fluctuates in the range of $[-38.43, -0.9]$ dB for $N = 251$, and $[-38.62, -10.26]$ dB for $N = 314$. The occurrence of these fluctuations is related to the Davies transformation. The range of azimuth HPBW for

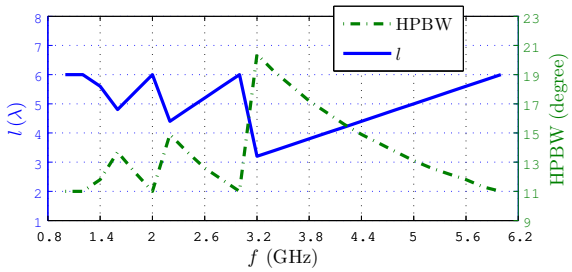

Fig. 8. The Inverse Proportionality of Elevation HPBW and ULA Electronic Aperture $l\,(\lambda)$ at $f = [1, 6]$ GHz

TABLE II
SIMULATION RESULTS FOR UCA IN 1 GHZ FREQUENCY

d_{C} (λ)	d_{C} (cm)	N	N_{V}	r_{C} (cm)	HPBW (degree)	μ_{MSLL} (dB)
0.03	1	314	27	49.97	16.6	-38.6
0.04	1.25	251	27	49.93	16.6	-38.5
0.05	1.5	210	27	50.13	16.6	-38.4
0.1	3	106	27	50.61	16.6	-37.9
0.2	6	53	27	50.61	16.6	-37.1
0.3	9	35	27	50.13	16.6	-36.4
0.4	12	26	21	49.66	21.4	-34.4
0.5	15	21	13	50.13	35	-33.9

TABLE III
SIMULATION RESULTS FOR UCA IN 6 GHZ FREQUENCY

d_C (λ)	d_C (cm)	N	N_V	r_C (cm)	HPBW (degree)	μ_{MSLL} (dB)
0.2	1	314	137	49.97	3	-20.1
0.25	1.25	251	137	49.93	3.1	-26.4
0.3	1.5	209	137	49.89	3.1	-10
0.35	1.75	179	137	49.86	3.1	-0.3
0.4	2	157	137	49.97	3.1	-17.1
0.45	2.25	139	137	49.78	3.1	-21
0.5	2.5	125	119	49.74	3.54	-18

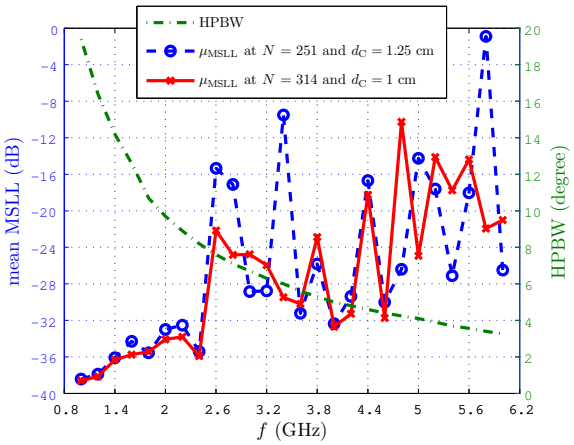

Fig. 9. Azimuth MSLL and HPBW at $N = 251$ and $N = 314$

both parameters is $[3.26°, 19.4°]$. Narrower HPBW is observed in the higher frequency due to larger electronic aperture.

From these results, the circular aperture of $r_C = 0.5$ m should be measured in 314 points, each 1 cm apart. All samples will be used for the data analysis (beam-forming) with the corresponding $N_V(f)$, so that $J_H(kr_C) \geq 0.1$.

The fluctuations observed in Fig. 9 occured due to the Davies transformation. It was shown in (6) that the normalizer diagonal matrix is composed of Bessel functions of the first kind, $J_h(kr_C)$, as the denominator. The order h is related to the number of virtual array elements, where h = -H, ..., 0, ..., H, and $H = \frac{N_V-1}{2}$. The argument kr_C is a function of frequency and array radius, which is relatively fixed at $r_C \simeq 0.5$ m. Thus, in a fixed frequency, Bessel function argument is relatively fixed at around $kr_C = 10\pi/3$ for $f = 1$ GHz, and around $kr_C = 20\pi$ for $f = 6$ GHz. For a fixed argument, the Bessel function of the first kind fluctuates and will asymptotically goes to zero with the increase of its order. When $J_h(kr_C) \simeq 0$, the weighting value will go to infinity, i.e. super-directivity. In the simulation, N_V was chosen such that $J_H(kr_C) \geq 0.1$. However, due to the fluctuation characteristic of Bessel Function, at certain frequencies and certain h, $J_h(kr_C) \simeq 0$. Fig. 10 shows that azimuth MSLL peaks occur when $J_h(kr_C) \simeq 0$.

In the case of ULA, the physical height, l, can be decreased by taking fewer samples of the total measurements. However, different from ULA, the physical radius of UCA, r_C, cannot be decreased. The reason is because one same measurement scheme is required for all measurement frequencies of $f = [1, 6]$ GHz, and at $f = 1$ GHz, maximum aperture is preferred to obtain a reasonable HPBW.

IV. CONCLUSIONS AND FUTURE WORK

The SAC evaluation by a synthetic cylindrical array beam-forming is proposed. The influence of elements position-error on

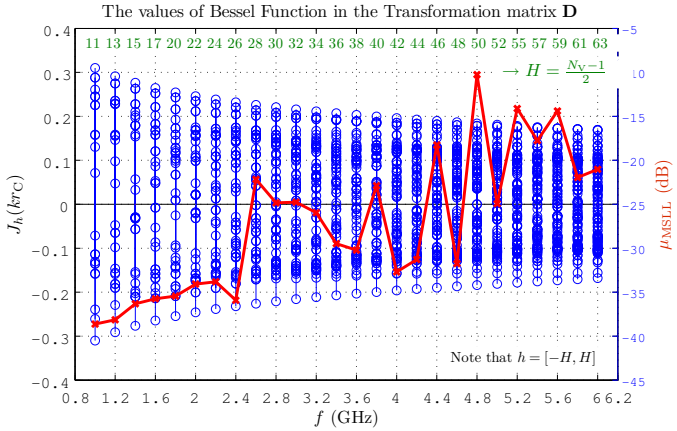

Fig. 10. Fluctuation of Azimuth MSLL and the Values of $J_h(kr_C)$

the performance of the array antenna was investigated by beam-forming simulations. It was found that the optimal geometry of synthetic cylindrical array antenna measurement for SAC evaluation is 1.8 m height and 1 m diameter, with 2.5 cm (linear) and 1 cm (circular) interelement spacings.

In the data analysis, each frequency will be separately analyzed by using 13 linear samples with a corresponding $d_L(f)$, and all circular samples with a corresponding $N_V(f)$. Utilizing this scheme, the expected array performance under the influence of Gaussian elements position-error with standard deviation of 1 mm (linear) and 0.1° (circular) are:

- Elevation MSLL = $[-36.8, -24.7]$ dB at HPBW = $[11°, 20.4°]$.
- Azimuth MSLL = $[-38.6, -10.3]$ dB at HPBW = $[3.3°, 19.4°]$.

The overall simulation results reveal the trade-off between MSLL (sensitivity) and HPBW (resolution), as well as the trade-off between HPBW and aperture size.

In the future, the fluctuation in azimuth MSLL may be compensated by taking additional samplings at a smaller radius, to be used at the higher frequency. However, this will results in a longer measurement time and widening of HPBW. The far-field assumption taken in this study should also be justified by using spherical-wave propagation, since the relative size of the SAC and that of the array may not satisfy this assumption.

REFERENCES

[1]CISPR 16-1-4, "Specification for Radio Disturbance and Immunity Measuring Apparatus and Methods – Part 1-4: Radio Disturbance and Immunity Measuring Apparatus – Antennas and Test Sites for Radiated Disturbance Measurements", Edition 3.0, April 2010.

[2]C. L. Holloway, and E. F. Kuester, "Modeling Semi-Anechoic Electromagnetic Measurement Chambers", *IEEE Trans. Electromagnetic Compatibility*, vol. 38, no. 1, pp. 79-84, February 1996.

[3]C. L. Dolph, "A current distribution for broadside arrays which optimizes the relationship between beam width and sidelobe level," *Proc. of the I.R.E. and Waves and Electrons*, pp. 335–348, June 1946.

[4]D. E. N. Davies, "A transformation between the phasing techniques required for linear and circular aerial arrays," *Proc. IEE*, vol. 112, no. 11, pp. 2041–2045, November 1965.

[5]M. Wax, and J. Sheinvald, "Direction finding of coherent signals via spatial smoothing for uniform circular arrays," *IEEE Trans. Antennas and Propagation*, vol. 42, no. 5, pp. 613-620, May 1994.

[6]M. Ghoraishi, J. Takada, A. Nishihara, and T. Imai, "Optimum Beamforming for Arbitrary Array Antenna", *IEICE Technical Report*, A·P2008-137, November 2008.

[7]B. K. Lau, and Y. H. Leung, "A Dolph-Chebyshev approach to the synthesis of array patterns for uniform circular arrays", *IEEE International Symposium on Circuits and Systems*, vol. I, pp. 124–127, May 2000.